A survey on wavelet methods for (geo) applications

Willi FREEDEN, Thorsten MAIER, Steffen ZIMMERMANN

University of Kaiserslautern
Geomathematics Group
D-67653 Kaiserslautern
P.O.Box 3049 Germany
freeden@mathematik.uni-kl.de

Recibido: 29 de Enero de 2002
Aceptado: 27 de Junio de 2002

ABSTRACT

Wavelets originated in 1980's for the analysis of (seismic) signals and have seen an explosion of applications. However, almost all the material is based on wavelets over Euclidean spaces. This paper deals with an approach to the theory and algorithmic aspects of wavelets in a general separable Hilbert space framework. As examples Legendre wavelets on the interval $[-1,+1]$ and scalar and vector spherical wavelets on the unit sphere Ω are discussed in more detail.

2000 Mathematics Subject Classification: 65T60, 65Z05, 42C40, 86A25.
Key words: Wavelet theory, scalar multiscale approximation,
vectorial multiscale approximation, pyramid scheme, geoapplications.

1. Introduction

Wavelets form "building blocks" that enable fast decorrelation of data. In other words, three features are incorporated in this way of thinking about wavelets, namely basis property, decorrelation, and fast computation. In the first part of the paper we discuss these aspects in a separable (functional) Hilbert space setup. As an essential tool we assume an orthonormal Hilbert basis to be known. The definitions of scaling function and wavelet are based on the concept of product kernels in terms of the prescribed orthonormal Hilbert basis. By virtue of the *basis property* each signal, i.e. each member of the Hilbert space, can be expressed in stable way as linear combination of dilated and shifted copies of a "mother kernel" with vanishing zeroth moment. The wavelet transform maps members of the Hilbert space into an associated two-parameter class of space and scale dependent elements. Wavelets show

ISSN: 1139-1138
http://dx.doi.org/10.5209/rev_REMA.2003.v16.n1.16879

the power of *decorrelation*. As a consequence the representation of the data in terms of wavelets is somehow "more compact" than the original representation, that is to say, we search for an accurate approximation by only using a small fraction of the original information of an element of the Hilbert space. Typically, in the jargon of information theory, scaling functions provide lowpass filtering, while the decorrelation is achieved by building wavelets which decay towards low and high frequencies, i.e. by bandpass filtering. Finally, the main question in wavelet approximation is how to decompose a function into wavelet coefficients, and how to reconstruct efficiently the function under consideration from the wavelet coefficients. There is a *tree algorithm*, i.e. a pyramid scheme, that makes these steps simple and fast. The fast decorrelation power of wavelets is the key to applications such as data compression, fast data transmission, noise cancellation, etc.

2. $\mathcal{H}$–Fourier expansions

Let $\mathcal{H}$ be a separable real functional Hilbert space over a certain domain $\Sigma \subset \mathbb{R}^n$ equipped with the inner product $(\cdot,\cdot)_{\mathcal{H}}$, i.e. $(\mathcal{H},(\cdot,\cdot)_{\mathcal{H}})$ is a Hilbert space consisting of functions $F : \Sigma \to \mathbb{R}$. Furthermore, let $\{U_n^*\}_{n=0,1,\ldots}$ be a (known) complete orthonormal system in $(\mathcal{H},(\cdot,\cdot)_{\mathcal{H}})$.

In a separable real functional Hilbert space $(\mathcal{H},(\cdot,\cdot)_{\mathcal{H}})$ any function $F \in \mathcal{H}$ can be represented as a *Fourier expansion* relative to the orthonormal system $\{U_n^*\}_{n=0,1,\ldots}$ (in the sense of $\|\cdot\|_{\mathcal{H}}$) by

$$F = \sum_{n=0}^{\infty} F^{\wedge}(n) U_n^* \tag{1}$$

with "*Fourier transforms*" (coefficients)

$$F^{\wedge}(n) = (F, U_n^*)_{\mathcal{H}}, \quad n = 0,1,2,\ldots . \tag{2}$$

Fourier expansions (1) are very successful at picking out "frequencies" n from a signal (function) $F \in \mathcal{H}$, but the use of non–space localizing functions U_n^* is incapable of dealing properly with data changing on small spatial scales. Usually a signal (function) refers to a certain combination of frequencies, and the frequencies themselves are spatially changing. This space evolution of the frequencies is not reflected in a Fourier series (1) of non–space localizing (for example, polynomial) trial functions U_n^* on Σ. With wavelets, as we are going to show in the next chapters, the amount of localization in space and in frequency is automatically adapted. The basic framework of this idea is based on convolving the signal (function) against "dilated" and "shifted" versions of the "mother (wavelet) kernel". Essential tools are the concepts of $\mathcal{H}$–product–kernels and $\mathcal{H}$–convolutions (cf. [12]).

3. $\mathcal{H}$–Product kernels

Any function $\Gamma : \Sigma \times \Sigma \to \mathbb{R}$ of the form

$$\Gamma(x,y) = \sum_{n=0}^{\infty} \Gamma^{\wedge}(n) U_n^*(x) U_n^*(y), \qquad x,y \in \Sigma, \tag{3}$$

with $\Gamma^{\wedge}(n) \in \mathbb{R}$, $n \in \mathbb{N}_0$, is called an *$\mathcal{H}$-product kernel* (briefly called $\mathcal{H}$-kernel). The sequence $\{\Gamma^{\wedge}(n)\}_{n=0,1,\ldots}$ is called the *symbol of the $\mathcal{H}$-kernel* (3).

Definition 1. *A symbol $\{\Gamma^{\wedge}(n)\}_{n=0,1,\ldots}$ of an $\mathcal{H}$-product kernel (3) is said to be $\mathcal{H}$-admissible if it satisfies the following conditions:*

$$(i) \quad \sum_{n=0}^{\infty} \left(\Gamma^{\wedge}(n)\right)^2 < \infty, \qquad (ii) \quad \sum_{n=0}^{\infty} \left(\Gamma^{\wedge}(n) U_n^*(x)\right)^2 < \infty \tag{4}$$

for all $x \in \Sigma$.

4. $\mathcal{H}$–Convolutions

$\mathcal{H}$-convolutions will be introduced in the following way.

Definition 2. *Let F be of class $\mathcal{H}$. Suppose that Γ is an $\mathcal{H}$-kernel of the form (3) with $\mathcal{H}$-admissible symbol $\{\Gamma^{\wedge}(n)\}_{n=0,1,\ldots}$, then the convolution of Γ against F is defined by*

$$(\Gamma *_{\mathcal{H}} F)(x) = (\Gamma(x,\cdot), F)_{\mathcal{H}} = \sum_{n=0}^{\infty} \Gamma^{\wedge}(n) F^{\wedge}(n) U_n^*(x). \tag{5}$$

From (5) we immediately see that

$$(\Gamma *_{\mathcal{H}} F)^{\wedge}(n) = \Gamma^{\wedge}(n) F^{\wedge}(n), \qquad n \in \mathbb{N}_0. \tag{6}$$

The convolution of two $\mathcal{H}$-product kernels with $\mathcal{H}$-admissible symbols leads to the following result.

Theorem 1. *Let Γ_1 and Γ_2 be $\mathcal{H}$-kernels with $\mathcal{H}$-admissible symbols $\{\Gamma_1^{\wedge}(n)\}_{n=0,1,\ldots}$ and $\{\Gamma_2^{\wedge}(n)\}_{n=0,1,\ldots}$, respectively. Then*

$$\begin{aligned} (\Gamma_1 *_{\mathcal{H}} \Gamma_2)(x,y) &= (\Gamma_1 *_{\mathcal{H}} \Gamma_2(\cdot,y))(x) \\ &= (\Gamma_1(x,\cdot), \Gamma_2(\cdot,y))_{\mathcal{H}} \\ &= \sum_{n=0}^{\infty} \Gamma_1^{\wedge}(n) \Gamma_2^{\wedge}(n) U_n^*(x) U_n^*(y) \end{aligned}$$

holds for all $x,y \in \Sigma$, and the sequence $\{(\Gamma_1 *_{\mathcal{H}} \Gamma_2)^{\wedge}(n)\}_{n=0,1,\ldots}$ given by

$$(\Gamma_1 *_{\mathcal{H}} \Gamma_2)^{\wedge}(n) = \Gamma_1^{\wedge}(n) \Gamma_2^{\wedge}(n) \tag{7}$$

constitutes an $\mathcal{H}$-admissible symbol of the $\mathcal{H}$-kernel $\Gamma_1 *_{\mathcal{H}} \Gamma_2$.

5. $\mathcal{H}$-Scaling functions

After having explained the convolution between two $\mathcal{H}$-kernels with $\mathcal{H}$-admissible symbols we are now interested in developing countable families $\{\Gamma_J\}$, $J \in \mathbb{Z}$, of $\mathcal{H}$-product kernels Γ_J which may be understood as scaling functions in our general Hilbert $\mathcal{H}$-wavelet concept.

As preparation we introduce a dilation operator acting on these families in the following way: Let Γ_J be a member of the family of product kernels. Then the *dilation operator* D_k, $k \in \mathbb{Z}$, is defined by $D_k\Gamma_J = \Gamma_{J+k}$. In particular, we have $\Gamma_J = D_J\Gamma_0$. Thus we refer to Γ_0 as the "mother kernel". Moreover, we define a *shifting operator* S_x, $x \in \Sigma$, $J \in \mathbb{Z}$, by $S_x\Gamma_J = \Gamma_J(x,\cdot)$. In doing so we consequently get by composition the operator $\Gamma_J(x,\cdot) = S_xD_J\Gamma_0$ for all $x \in \Sigma$ and all $J \in \mathbb{Z}$. Note that all kernels Γ_J are symmetric, so that $\Gamma_J(x,y) = \Gamma_J(y,x)$, $x,y \in \Sigma$, for all $J \in \mathbb{Z}$.

We are now in position to introduce scaling functions.

Definition 3. *Let $\{(\Phi_J)^\wedge(n)\}_{n=0,1,\dots}$, $J \in \mathbb{Z}$, define an $\mathcal{H}$-admissible symbol of a family of $\mathcal{H}$-kernels satisfying additionally the following properties:*

$$
\begin{aligned}
&(i) && \lim_{J\to\infty} \left((\Phi_J)^\wedge(n)\right)^2 = 1\ , && n \in \mathbb{N},\\
&(ii) && \left((\Phi_J)^\wedge(n)\right)^2 \geq \left((\Phi_{J-1})^\wedge(n)\right)^2\ , && J \in \mathbb{Z},\ n \in \mathbb{N}\ ,\\
&(iii) && \lim_{J\to-\infty} \left((\Phi_J)^\wedge(n)\right)^2 = 0, && n \in \mathbb{N}\ ,\\
&(iv) && ((\Phi_J)^\wedge(0))^2 = 1\ , && J \in \mathbb{Z}\ .
\end{aligned}
$$

Then $\left\{(\Phi_J)^\wedge(n)\right\}_{n=0,1,\dots}$ is called the generating symbol of an $\mathcal{H}$-scaling function. The family of $\mathcal{H}$-kernels $\{\Phi_J\}$, $J \in \mathbb{Z}$, given by

$$\Phi_J(x,y) = \sum_{n=0}^{\infty} (\Phi_J)^\wedge(n) U_n^*(x) U_n^*(y), \qquad x,y \in \Sigma\ , \tag{8}$$

is called $\mathcal{H}$-scaling function.

The $\mathcal{H}$–scaling functions constructed in this way, therefore, satisfy the essential conditions of the classical wavelet concept (see e.g. [5, 11]). From the results of the previous chapter it follows immediately that $\Phi_J(x,\cdot)$, $x \in \Sigma$, $J \in \mathbb{Z}$, is a member of $\mathcal{H}$. It can be easily seen that $\Phi_J^{(2)} = \Phi_J *_{\mathcal{H}} \Phi_J$, $J \in \mathbb{Z}$, is an $\mathcal{H}$-kernel with $\mathcal{H}$-admissible symbol $\left\{((\Phi_J)^\wedge(n))^2\right\}$, $n = 0,1,\dots$.

This leads us to the following central result in the theory of $\mathcal{H}$–scaling functions.

Theorem 2. *Let $\{(\Phi_J)^\wedge(n)\}_{n=0,1,\dots}$, $J \in \mathbb{Z}$, be the generating symbol of a scaling function $\{\Phi_J\}$. Then*

$$\lim_{J\to\infty} \|F_J - F\|_{\mathcal{H}} = 0 \tag{9}$$

holds for all $F \in \mathcal{H}$, where F_J given by

$$F_J = \Phi_J^{(2)} *_{\mathcal{H}} F = (\Phi_J *_{\mathcal{H}} \Phi_J) *_{\mathcal{H}} F \ , \qquad F \in \mathcal{H} \tag{10}$$

is said to be the J-level approximation of F.

Proof. We introduce the operator $T_J : \mathcal{H} \to \mathcal{H}$, $J \in \mathbb{Z}$, by

$$F_J = T_J F = (\Phi_J *_{\mathcal{H}} \Phi_J) *_{\mathcal{H}} F. \tag{11}$$

From the definition of the convolution and the fact that $\Phi_J^{(2)} = \Phi_J *_{\mathcal{H}} \Phi_J$ is an $\mathcal{H}$-kernel with $\mathcal{H}$-admissible symbol it follows that $T_J F$ can be written as follows:

$$T_J F = \sum_{n=0}^{\infty} ((\Phi_J)^\wedge(n))^2 F^\wedge(n) U_n^* \ . \tag{12}$$

But this implies that

$$\begin{aligned} \|T_J\| &= \sup_{\substack{G \in \mathcal{H} \\ \|G\|_{\mathcal{H}}=1}} \|T_J G\|_{\mathcal{H}} \qquad (13) \\ &= \left(\sum_{n=0}^{\infty} ((\Phi_J)^\wedge(n))^4 (G^\wedge(n))^2 \right)^{\frac{1}{2}} \\ &\leq \sup_{n \in \mathbb{N}_0} ((\Phi_J)^\wedge(n))^2 \left(\sum_{n=0}^{\infty} (G^\wedge(n))^2 \right)^{\frac{1}{2}} \\ &\leq \sup_{n \in \mathbb{N}_0} ((\Phi_J)^\wedge(n))^2 < \infty \end{aligned}$$

for every $J \in \mathbb{Z}$, since $\{(\Phi_J)^\wedge(n)\}_{n=0,1,\ldots}$, $J \in \mathbb{Z}$, is $\mathcal{H}$-admissible.

Now, from Parseval's identity, we obtain

$$\lim_{J \to \infty} \|T_J F - F\|_{\mathcal{H}}^2 = \lim_{J \to \infty} \sum_{n=0}^{\infty} (1 - ((\Phi_J)^\wedge(n))^2)^2 (F^\wedge(n))^2. \tag{14}$$

From the conditions (i), (ii) and (iv) of Definition 3 we are able to deduce that $((\Phi_J)^\wedge(n))^2 \leq 1$ for $n \in \mathbb{N}_0$. But this shows us that

$$0 \leq (1 - ((\Phi_J)^\wedge(n))^2)^2 \leq 1 \tag{15}$$

is valid for all $n \in \mathbb{N}_0$. Therefore, the limit and the infinite sum in (14) may be interchanged. By applying (i) and (iv) we finally arrive at the desired result. ■

6. $\mathcal{H}$–Multiresolution analysis

Note that condition (iii) of Definition 3 has not been used yet. This condition, however, is needed as assumption for defining $\mathcal{H}$-wavelets and establishing a multiresolution analysis as will be explained now.

According to our construction, for any $F \in \mathcal{H}$, each $T_J F$ defined by (11) provides an approximation of F at scale J. In terms of filtering the product kernels $\Phi_J^{(2)} = \Phi_J *_{\mathcal{H}} \Phi_J$ may be interpreted as low-pass filter. T_J is the convolution operator of this low-pass filter. Accordingly we understand the *scale space* $\mathcal{V}_J$ to be the image of $\mathcal{H}$ under the operator T_J:

$$\mathcal{V}_J = T_J(\mathcal{H}) = \{(\Phi_J *_{\mathcal{H}} \Phi_J) *_{\mathcal{H}} F \mid F \in \mathcal{H}\}. \tag{16}$$

As an immediate consequence we obtain the following result.

Theorem 3. *The scale spaces satisfy the following properties:*

$$(i) \qquad \{U_0^*\} \subset \mathcal{V}_J \subset \mathcal{V}_{J'} \subset \mathcal{H}\ , \qquad J \leq J', \tag{17}$$

$$(ii) \qquad \bigcap_{J=-\infty}^{\infty} \mathcal{V}_J = \{U_0^*\}, \tag{18}$$

$$(iii) \qquad \overline{\bigcup_{J=-\infty}^{\infty}}^{\|\cdot\|_{\mathcal{H}}} = \mathcal{H}, \tag{19}$$

$$(iv) \qquad \text{if } F_J \in \mathcal{V}_J \text{ then } D_{-1} F_J \in \mathcal{V}_{J-1}, \qquad J \in \mathbb{Z}. \tag{20}$$

Proof. From the conditions (ii) and (iv) of Definition 3 we easily get the validity of the first assertion (17) of Theorem 3. The identity (18) follows directly from the conditions (iii) and (iv) of Definition 3. The formula (19) is a consequence of Theorem 2, while (20) follows immediately from the definition of the shifting operator D_J. ■

If a collection of subspaces of $\mathcal{H}$ satisfies the conditions of Theorem 3, it is called a *$\mathcal{H}$–multiresolution analysis* (MRA).

7. $\mathcal{H}$-wavelets

The definition of the scaling functions now allows us to introduce $\mathcal{H}$-wavelets. Basic tool again is the concept of $\mathcal{H}$-product kernels. We start with the definition of wavelets by aid of a "refinement (scaling) equation".

Definition 4. *Let $\{(\Phi_J)^\wedge(n)\}_{n=0,1,\ldots}$, $J \in \mathbb{Z}$, be the generating symbol of an $\mathcal{H}$-scaling function as defined by Definition 3. Then the generating symbol $\{(\Psi_j)^\wedge(n)\}_{n=0,1,\ldots}$, $j \in \mathbb{Z}$, of the associated $\mathcal{H}$-wavelet is defined via the "refinement equation"*

$$(\Psi_j)^\wedge(n) = (((\Phi_{j+1})^\wedge(n))^2 - ((\Phi_j)^\wedge(n))^2)^{\frac{1}{2}}. \tag{21}$$

The family $\{\Psi_j\}$, $j \in \mathbb{Z}$, *of* $\mathcal{H}$*–product kernels given by*

$$\Psi_j(x,y) = \sum_{n=0}^{\infty} (\Psi_j)^\wedge(n) U_n^*(x) U_n^*(y), \qquad x, y \in \Sigma, \tag{22}$$

is called $\mathcal{H}$*-wavelet associated to the* $\mathcal{H}$*-scaling function* $\{\Phi_J\}$, $J \in \mathbb{Z}$. *The corresponding "mother wavelet" is denoted by* Ψ_0.

Note that the defining properties of an $\mathcal{H}$–wavelet presume the zero–mean property $(\Psi_j)^\wedge(0) = 0$, $j \in \mathbb{Z}$, i.e. the vanishing of the symbol element at 0. The wavelets constructed in this way, therefore, satisfy a substantial condition of the classical wavelet theory (see e.g. [5, 11]).

A dilation and a shifting operator can be understood in the same way as we did before. In other words, any wavelet can be interpreted as a dilated and shifted copy of the corresponding mother wavelet like $\Psi_j(x,\cdot) = S_x D_j \Psi_0(\cdot,\cdot)$. We can easily derive from the telescoping character of (21) that

$$\begin{aligned} ((\Phi_{J+1})^\wedge(n))^2 &= \sum_{j=-\infty}^{J} ((\Psi_j)^\wedge(n))^2 \\ &= ((\Phi_0)^\wedge(n))^2 + \sum_{j=0}^{J} ((\Psi_j)^\wedge(n))^2 \ . \end{aligned} \tag{23}$$

Similar to the definition of the operator T_j, $j \in \mathbb{Z}$, we are now led to the convolution operators $R_j : \mathcal{H} \to \mathcal{H}$ given by

$$R_j F = \Psi_j^{(2)} *_{\mathcal{H}} F = (\Psi_j *_{\mathcal{H}} \Psi_j) *_{\mathcal{H}} F, \qquad F \in \mathcal{H}. \tag{24}$$

Thus the identity

$$\Phi_{J+1} *_{\mathcal{H}} \Phi_{J+1} = \sum_{j=-\infty}^{J} (\Psi_j *_{\mathcal{H}} \Psi_j) = \Phi_0 *_{\mathcal{H}} \Phi_0 + \sum_{j=0}^{J} (\Psi_j *_{\mathcal{H}} \Psi_j) \tag{25}$$

can be written in operator formulation as follows:

$$T_{J+1} = \sum_{j=-\infty}^{J} R_j = T_0 + \sum_{j=0}^{J} R_j. \tag{26}$$

The convolution operators R_j describe the "detail information" of F at scale j. In terms of filtering, $\Psi_j^{(2)} = \Psi_j *_{\mathcal{H}} \Psi_j$, $j \in \mathbb{Z}$, may be interpreted as a band-pass filter. This fact immediately gives rise to introduce the *detail spaces* as follows:

$$\mathcal{W}_j = R_j(\mathcal{H}) = \{(\Psi_j *_{\mathcal{H}} \Psi_j) *_{\mathcal{H}} F \mid F \in \mathcal{H}\}. \tag{27}$$

$\mathcal{W}_J$ contains the "detail information" needed to go from an approximation at level J to an approximation at level $J+1$. Hence we get

$$\sum_{j=-\infty}^{J} \mathcal{W}_j = \mathcal{V}_0 + \sum_{j=0}^{J} \mathcal{W}_j = \mathcal{V}_{J+1}, \qquad \mathcal{V}_J + \mathcal{W}_J = \mathcal{V}_{J+1}, \qquad J \in \mathbb{Z}\,. \tag{28}$$

It should be noted that, in general, the sum in (28) is neither direct nor orthogonal. But there exist examples leading to an orthogonal multiresolution which should be discussed later on.

In conclusion, any $F \in \mathcal{H}$ can be approximated as follows: Starting with T_0F we find in connection to (26) by adding successively $R_0F, \ldots, R_JF$ the $(J+1)$–level approximation $T_{J+1}F$ of $F \in \mathcal{H}$. Obviously, the partial "reconstruction" R_jF is nothing else than the "difference of two smoothings" at two consecutive scales $R_jF = T_{j+1}F - T_jF$.

Definition 5. *The wavelet transform WT at scale $j \in \mathbb{Z}$ and position $x \in \Sigma$ is given by*

$$WT(F)(j;x) = (\Psi_j(x,\cdot), F)_{\mathcal{H}}, \qquad F \in \mathcal{H}. \tag{29}$$

Combining (29) and (25) we can formulate the main result of our wavelet theory as follows.

Theorem 4. *Let $\{(\Phi_J)^\wedge(n)\}_{n=0,1,\ldots}$, $J \in \mathbb{Z}$, be the generating symbol of an $\mathcal{H}$-scaling function. Suppose that $\{(\Psi_j)^\wedge(n)\}_{n=0,1,\ldots}$, $j \in \mathbb{Z}$, is the generating symbol of the corresponding $\mathcal{H}$-wavelet. Furthermore, let F be of class $\mathcal{H}$. Then*

$$F_J = (\Phi_0 *_{\mathcal{H}} \Phi_0) *_{\mathcal{H}} F + \sum_{j=0}^{J-1} \Psi_j *_{\mathcal{H}} (WT(F)(j,\cdot)) \tag{30}$$

is the J-level approximation of F satisfying

$$\lim_{J\to\infty} \|F_J - F\|_{\mathcal{H}} = 0. \tag{31}$$

The limit relation (31) shows the essential characteristic of wavelets. We change the approximated solution from F_J to F_{J+1} by adding the so-called detail information of level J as the difference of two smoothings of two consecutive scales J and $J+1$ and, what is more important, we are able to guarantee $\lim_{J\to\infty} F_J = F$ in the sense of the $\|\cdot\|_{\mathcal{H}}$-topology provided that $F \in \mathcal{H}$.

The following scheme briefly summarizes the essential steps of our wavelet approach in the framework of product kernels introduced for a separable functional Hilbert space $\mathcal{H}$.

$$\begin{array}{ccccccccccccc}
T_0F & & T_1F\ldots & & & & T_jF & & T_{j+1}F\ldots & \overset{j\to\infty}{\to} & F \\
\cap & & \cap & & & & \cap & & \cap & & \cap \\
\mathcal{V}_0 & \subset & \mathcal{V}_1 & \ldots & & \subset & \mathcal{V}_j & \subset & \mathcal{V}_{j+1} & \ldots = & \mathcal{H} \\
\mathcal{V}_0 & + \mathcal{W}_0 & + & \ldots + & \mathcal{W}_{j-1} & + & \mathcal{W}_j & + & \ldots & = & \mathcal{H} \\
\cup & \cup & & & \cup & & \cup & & & & \cup \\
T_0F & + R_0F & + & \ldots + & R_{j-1}F & + & R_jF & + & \ldots & = & F.
\end{array}$$

8. $\mathcal{H}$–Bandlimited wavelets

For simplicity, we assume that $\{\Phi_j\}_{j\in\mathbb{Z}}$ is a family of bandlimited kernels such that $((\Phi_j)^\wedge(n))^2 > 0$ for $n = 0, \ldots, N_j = 2^j - 1$ and $((\Phi_j)^\wedge(n))^2 = 0$ for $n \geq N_j + 1 = 2^j$. Then it follows that

$$\Phi_j(x,\cdot) \in \mathcal{H}_{0,\ldots,2^j-1} = \text{span}\{U_0^*, \ldots, U_{2^j-1}^*\} \tag{32}$$

and

$$\Psi_j(x,\cdot) \in \mathcal{H}_{0,\ldots,2^{j+1}-1} = \text{span}\{U_0^*, \ldots, U_{2^{j+1}-1}^*\} \tag{33}$$

holds for all $x \in \Sigma$, ("span" means, as usual, the set of all finite linear combinations). More explicitly,

$$\Phi_j(x,y) = \sum_{n=0}^{2^j-1} (\Phi_j)^\wedge(n) U_n^*(x) U_n^*(y), \tag{34}$$

$$\Psi_j(x,y) = \sum_{n=0}^{2^{j+1}-1} (\Psi_j)^\wedge(n) U_n^*(x) U_n^*(y) \tag{35}$$

for $(x,y) \in \Sigma \times \Sigma$. Consequently, the scale spaces and the detail spaces, respectively, fulfill the relations $\mathcal{V}_j = \mathcal{H}_{0,\ldots,2^j-1}$, $\mathcal{W}_j \subset \mathcal{H}_{0,\ldots,2^{j+1}-1}$.

Simple examples are given below:

(a) *orthogonal (Shannon) scaling function*

$$(\Phi_j)^\wedge(n) = \begin{cases} 1 & for \quad n = 0, \ldots, N_j \\ 0 & for \quad n \geq N_j + 1 \end{cases}, \tag{36}$$

(b) *non-orthogonal (smoothed Shannon) scaling function*

$$(\Phi_j)^\wedge(n) = \begin{cases} 1 & for \quad n = 0, \ldots, 2^j h \\ \frac{1-2^{-j}n}{1-h} & for \quad n = 2^j h, \ldots, N_j \\ 0 & for \quad n \geq N_j + 1 \end{cases} \tag{37}$$

for fixed $h \in [0,1)$,

(c) *non-orthogonal cubic polynomial (CP-) scaling function*

$$(\Phi_j)^\wedge(n) = \begin{cases} (1-2^{-j}n)^2(1+2^{-j+1}n) & for \quad n=0,\dots,N_j \\ 0 & for \quad n \geq N_j+1 \end{cases} \tag{38}$$

with

$$N_j = \begin{cases} 0 & for \quad j \in \mathbb{Z},\ j<0 \\ 2^j-1 & for \quad j \in \mathbb{Z},\ j \geq 0 \end{cases}. \tag{39}$$

Note that the case (a) leads to an orthogonal multiresolution analysis, i.e. the detail and the scale spaces satisfy $\mathcal{V}_{j+1} = \mathcal{V}_j \oplus \mathcal{W}_j$, $\mathcal{W}_j \perp \mathcal{W}_k$, $k \neq j$, $j \geq 0$. In the cases (b) and (c) the scale and detail spaces are still finite-dimensional, but the detail spaces are no longer orthogonal.

It should be noted that each scale space $\mathcal{V}_j$, $j \in \mathbb{N}_0$, can be understood as a finite dimensional reproducing Hilbert space with the inner product $(\cdot,\cdot)_{\mathcal{H}}$ and the (Shannon) reproducing kernel $(SH)_{N_j}$ being canonically defined by

$$(F,G)_{\mathcal{H}} = \sum_{n=0}^{N_j} F^\wedge(n)G^\wedge(n), \quad F,G \in \mathcal{H}_{0,\dots,N_j} \tag{40}$$

and

$$(SH)_{N_j}(x,y) = \sum_{n=0}^{N_j} U_n^*(x)U_n^*(y), \quad x,y \in \Sigma, \tag{41}$$

respectively.

The reproducing property enabled [10, 11, 12] to develop different variants of tree algorithms (even for the non–bandlimited case [11]).

9. A tree algorithm

Until now efforts have been made to establish the basis property and the ability of bandpass filtering in terms of wavelets. Next we come to the third feature of wavelet approximation, viz. fast computation, which will be realized in form of a pyramid scheme for bandlimited wavelets.

Let the assumptions of Chapter 8 be satisfied, i.e. $\mathcal{V}_j = \mathcal{H}_{0,\dots,N_j}$, $\mathcal{W}_j \subset \mathcal{H}_{0,\dots,N_{j+1}}$. The key ideas of our fast evaluation method are based on the following observations:

(1) For some suitably large J, the scale space $\mathcal{V}_J$ is "sufficiently close" to $\mathcal{H}$. Consequently, for each $F \in \mathcal{H}$, the error between F and $\Phi_J^{(2)} *_{\mathcal{H}} F$ (understood in the $\|\cdot\|_{\mathcal{H}}$–topology) may be assumed to be negligible. This is the reason why F is supposed to be of class $\mathcal{V}_J$ for the remainder of this chapter.

(2) For $j = 0, \ldots, J$, consider sequences $Y_{L_j} = \{y_1^{L_j}, \ldots, y_{L_j}^{L_j}\}$ of L_j points $y_i^{L_j} \in \Sigma$, $i = 1, \ldots, L_j$, such that

$$\mathcal{V}_j = \mathcal{H}_{0,\ldots,N_j} = \operatorname{span}\left(\Phi_j^{(2)}(\cdot, y_1^{L_j}), \ldots, \Phi_j^{(2)}(\cdot, y_{L_j}^{L_j})\right) \tag{42}$$

(the existence of pointsets $Y_{L_j} \subset \Sigma$ fulfilling the desired property is well-known from interpolation theory (see, for example, [6])).

(3) The (Shannon) kernel functions $(SH)_{N_j} : \Sigma \times \Sigma \to \mathbb{R}$ introduced by (41) satisfy the properties

$$\Phi_j^{(2)} = \Phi_j^{(2)} *_{\mathcal{H}} (SH)_{N_j}, \quad j = 0, \ldots, J, \tag{43}$$

and

$$(SH)_{N_j} = (SH)_{N_J} *_{\mathcal{H}} (SH)_{N_j}, \quad j = 0, \ldots, J. \tag{44}$$

In conclusion, for $F \in V_J$, it follows that

$$\Phi_j^{(2)} *_{\mathcal{H}} F = \Phi_j^{(2)} *_{\mathcal{H}} \left((SH)_{N_j} *_{\mathcal{H}} F\right), \tag{45}$$

$j = 0, \ldots, J$. Hence, from (42) it is clear that there exist real coefficients $a_l^{L_j}$ such that

$$\Phi_j^{(2)} *_{\mathcal{H}} F = \Phi_j^{(2)} *_{\mathcal{H}} \left((SH)_{N_j} *_{\mathcal{H}} F\right) = \sum_{l=1}^{L_j} a_l^{L_j} \Phi_j^{(2)}(\cdot y_l^{L_j}) \tag{46}$$

$j = 0, \ldots, J$. There remains the question if we need to calculate the coefficients $a_l^{L_j}$ for all $j = 0, \ldots, J$ or if there exist pyramid schemes such that it suffices to find the coefficients for the largest scale J since the lower scale coefficients can be calculated recursively. Starting point for our considerations are discretizations of the convolutions, i.e. we assume that a table of coefficients $\{w_l^{L_j}\}$, $l = 1, \ldots, L_j$, $j = 0, \ldots, J$, is known (see the example in Chapter 10) such that

$$\Phi_j^{(2)} *_{\mathcal{H}} \left((SH)_{N_j} *_{\mathcal{H}} F\right) = \sum_{l=1}^{L_j} w_l^{L_j} \left((SH)_{N_j}(\cdot, y_l^{L_j}) *_{\mathcal{H}} F\right) \Phi_j^{(2)}(\cdot, y_l^{L_j}), \tag{47}$$

i.e.:

$$a_l^{L_j} = w_l^{L_j} (SH)_{N_j}(\cdot, y_l^{L_j}) *_{\mathcal{H}} F, \quad l = 1, \ldots, L_j. \tag{48}$$

The coefficients $w_l^{L_j}$, $l = 1, \ldots, L_j$, are stored elsewhere for $j = 0, \ldots, J$. It is worth mentioning that discretizing the convolutions usually can be done by means of so-called integration formulas; prominent examples are equidistributions or equiangular longitude-latitude grids on spherical surfaces (see e.g. [11] and the references therein.)

What we are going to realize is a *tree algorithm (pyramid scheme)* with the following ingredients: Starting from a sufficiently large J such that

$$\Phi_J^{(2)}(\cdot, y_l^{L_J}) *_{\mathcal{H}} F = \sum_{l=1}^{L_J} a_l^{L_J} \Phi_J^{(2)}(\cdot, y_l^{L_J}) \tag{49}$$

with

$$a_l^{L_J} = w_l^{L_J} (SH)_{N_J}(\cdot, y_l^{L_J}) *_{\mathcal{H}} F = w_l^{L_J} F(y_l^{L_J}), \quad l = 1, \ldots, L_J, \tag{50}$$

our aim is to show that the coefficient vectors $a^{L_j} = (a_1^{L_j}, \ldots, a_{L_j}^{L_j})^T \in \mathbb{R}^{L_j}$, $j = 0, \ldots, J-1$, given by (48) (and being, of course, dependent on the function $F \in V_J$ under consideration) can be calculated such that the following properties are true:

(i) The vectors a^{L_j}, $j = 0, \ldots, J-1$, are obtainable by recursion from the values a^{L_J}.

(ii) For $j = 0, \ldots, J$

$$\Phi_j^{(2)} *_{\mathcal{H}} F = \sum_{l=1}^{L_j} a_l^{L_j} \Phi_j^{(2)}(\cdot, y_l^{L_j}) \tag{51}$$

and for $j = 1, \ldots, J$

$$\Psi_{j-1}^{(2)} *_{\mathcal{H}} F = \sum_{l=1}^{L_j} a_l^{L_j} \Psi_{j-1}^{(2)}(\cdot, y_l^{L_j}). \tag{52}$$

Note that, if we can fulfill the second condition, we are able to calculate the convolutions with scaling functions as well as with wavelets from the same set of coefficients and, therefore, have found a recursion for the determination of the complete multiresolution analysis.

Our considerations are divided into two parts, viz. the initial step concerning the scale J and the pyramid step establishing the recursion relation:

The Initial Step. For suitably large J the formula (49) holds true with (50):

$$a_l^{L_J} = w_l^{L_J} F(y_l^{L_J}), \quad l = 1, \ldots, L_J\,. \tag{53}$$

The Pyramid Step. From (46) it follows immediately that

$$\left(\Phi_j^{(2)}\right)^{\wedge}(n) F^{\wedge}(n) = \sum_{l=1}^{L_j} a_l^{L_j} (\Phi_j^{(2)})^{\wedge}(n) U_n^*(y_l^{L_j}) \tag{54}$$

i.e.:

$$F^{\wedge}(n) = \sum_{l=1}^{L_j} a_l^{L_j} U_n^*(y_l^{L_j}) \tag{55}$$

for $n = 0, \dots, N_j$, i.e. the Fourier coefficient of the function under consideration is independent of the kernel functions involved. But this shows us that

$$K_j *_{\mathcal{H}} F = K_j *_{\mathcal{H}} \left((SH)_{N_j} *_{\mathcal{H}} F \right) = \sum_{l=1}^{L_j} a_l^{L_j} K_j(\cdot, y_l^{L_j}) \tag{56}$$

holds for all $\mathcal{H}$–product kernels $K_j : \Sigma \times \Sigma \to \mathbb{R}$ of the form

$$K_j(x,y) = \sum_{n=0}^{N_j} K_j^{\wedge}(n) U_n^*(x) U_n^*(y), \ (x,y) \in \Sigma \times \Sigma \tag{57}$$

with arbitrary (real) coefficients $K_j^{\wedge}(0), \dots, K_j^{\wedge}(N_j)$. In particular, we have

$$\Psi_{j-1} *_{\mathcal{H}} F = \Psi_{j-1} *_{\mathcal{H}} \left((SH)_{N_j} *_{\mathcal{H}} F \right) = \sum_{l=1}^{L_j} a_l^{L_j} \Psi_{j-1} \left(\cdot, y_l^{L_j} \right) \tag{58}$$

and

$$\Psi_{j-1}^{(2)} *_{\mathcal{H}} F = \Psi_{j-1}^{(2)} *_{\mathcal{H}} \left((SH)_{N_j} *_{\mathcal{H}} F \right) = \sum_{l=1}^{L_j} a_l^{L_j} \Psi_{j-1}^{(2)} \left(\cdot, y_l^{L_j} \right) \ . \tag{59}$$

Moreover, we find for $j = 1, \dots, J$

$$(SH)_{N_{j-1}} *_{\mathcal{H}} F = (SH)_{N_{j-1}} *_{\mathcal{H}} \left((SH)_{N_j} *_{\mathcal{H}} F \right) = \sum_{l=1}^{L_j} a_l^{L_j} (SH)_{N_{j-1}}(\cdot, y_l^{L_j}). \tag{60}$$

Now we obtain from (48) in connection with (60) the recursion relation

$$\begin{aligned} a_i^{L_{j-1}} &= w_i^{L_{j-1}} (SH)_{N_{j-1}}(\cdot, y_i^{L_{j-1}}) *_{\mathcal{H}} F \\ &= w_i^{L_{j-1}} \sum_{l=1}^{L_j} a_l^{L_j} (SH)_{N_{j-1}}(y_i^{L_{j-1}}, y_l^{L_j}), \end{aligned} \tag{61}$$

$j = 1, \dots, J$.

In other words, the coefficients $a_l^{L_{J-1}}$ can be calculated recursively starting from $a_l^{L_J}$ for the initial level J, $a_l^{L_{J-2}}$ can be deduced recursively from $a_l^{L_{J-1}}$ etc. Moreover it is worth mentioning that the coefficients are independent of the special choice of the wavelet. This finally leads us to the formulae

$$\Phi_j^{(2)} *_{\mathcal{H}} F = \sum_{l=1}^{L_j} a_l^{L_j} \Phi_j^{(2)}(\cdot, y_l^{L_j}), \quad j = 0, \dots, J \tag{62}$$

and

$$\Psi_{j-1}^{(2)} * F = \sum_{l=1}^{L_j} a_l^{L_j} \Psi_{j-1}^{(2)}(\cdot, y_l^{L_j}), \qquad j = 0, \dots, J \tag{63}$$

with coefficients given by (50) and (61). Furthermore, the coefficients $a_l^{L_j}$ can be used to calculate the wavelet transform $\Psi_{j-1} *_{\mathcal{H}} F$ for $j = 0, \dots, J-1$.

The recursion procedure leads us to the following *decomposition scheme*:

$$\begin{array}{ccccccccccc} F & \to & a^{L_J} & \to & a^{L_{J-1}} & \to & \dots & \to & a^{L_1} & \to & a^{L_0} \\ & & \downarrow & & \downarrow & & & & \downarrow & & \downarrow \\ & & \Psi_{J-1}^{(2)} *_{\mathcal{H}} F & & \Psi_{J-2}^{(2)} *_{\mathcal{H}} F & & & & \Psi_0^{(2)} *_{\mathcal{H}} F & & \Phi_0^{(2)} * F. \end{array} \tag{64}$$

The coefficient vectors $a^{L_0}, a^{L_1}, \dots$ allow the following *reconstruction scheme*:

$$\begin{array}{ccccccccccc} a^{L_0} & & & & a^{L_1} & & & & a_{L_2} & & \\ \downarrow & & & & \downarrow & & & & \downarrow & & \\ \Phi_0^{(2)} *_{\mathcal{H}} F & \to & + & \to & \Psi_0^{(2)} *_{\mathcal{H}} F & \to & + & \to & \Psi_1^{(2)} * F & \to & \dots \ . \\ & & & & \downarrow & & & & \downarrow & & \\ & & & & \Phi_1^{(2)} *_{\mathcal{H}} F & & & & \Phi_2^{(2)} *_{\mathcal{H}} F & & \end{array} \tag{65}$$

In the previous chapters we described wavelets as intimately related to a multiresolution analysis. Moreover, any bandlimited signal (function) is reconstructable by using bandlimited wavelets.

We saw that the multiresolution analysis "looks" at the signal through a microscope, whose resolution gets finer and finer. Thus it associates to the signal a sequence of smoothed versions, labelled by the scale parameter. The wavelets provide a powerful tool in interpreting and constructing lowpass and bandpass filters. This makes wavelets particularly useful for data compression. In fact, compression techniques aim at reducing storage requirements for the signal and at speeding up read or write operations. In case of compression we are ready to accept an error, for example, by using a threshold for the wavelet coefficients (see e.g. [7, 8, 14, 17]) as long as the quality after compression is acceptable.

10. Noise cancellation

Thus far only a deterministic function model has been used. If a comparison of a measured function with the actual value were done, a discrepancy would be observed. A mathematical description of this discrepancy has to follow the laws of probability theory in a stochastic model. Usually the observations are not looked upon as a time series but rather as a function $\tilde{F}$ ('~' for stochastic) for which it is canonical to assume that

$$\tilde{F} = F + \tilde{\varepsilon},$$

where $\tilde{\varepsilon}$ is the observation noise. Moreover, in our approach, we suppose the covariance to be known in the form

$$Cov[\tilde{F}(x), \tilde{F}(y)] = E[\tilde{\varepsilon}(x), \tilde{\varepsilon}(y)] = K(x,y), \quad (x,y) \in \Sigma \times \Sigma,$$

where $K : \Sigma \times \Sigma \to \mathbb{R}$ is an $\mathcal{H}$-kernel

$$K(x,y) = \sum_{n=0}^{\infty} K^{\wedge}(n) U_n^*(x) U_n^*(y), \quad (x,y) \in \Sigma \times \Sigma,$$

with $\mathcal{H}$-admissible symbol $\{K^{\wedge}(n)\}_{n=0,1,\ldots}$.

Since the large "true" coefficients are the ones that should be included in a selective reconstruction, in estimating an unknown function $F \in \mathcal{H}$, it is natural to include only coefficients larger than some specified threshold value. In our context a 'larger' coefficient is taken to mean one that satisfies for $j = 0, \ldots, J$ and $l = 1, \ldots, L_j$

$$\begin{aligned}
\left(\tilde{a}_l^{L_j}\right)^2 &= \left(w_l^{L_j} (SH)_{N_j}(\cdot, y_l^{N_j}) *_{\mathcal{H}} \tilde{F}\right)^2 \\
&= \left(w_l^{L_j}\right)^2 \left(\left(\tilde{F}(\cdot)\tilde{F}(\cdot), (SH)_{N_j}(\cdot, y_l^{N_j})\right)_{\mathcal{H}}, (SH)_{N_j}(\cdot, y_l^{Nj})\right)_{\mathcal{H}} \\
&\geq \left(w_l^{L_j}\right)^2 \left(\left(K(\cdot,\cdot), (SH)_{N_j}(\cdot, y_l^{N_j})\right)_{\mathcal{H}}, (SH)_{N_j}(\cdot, y_l^{N_j})\right)_{\mathcal{H}} \\
&= \left(k_l^{L_j}\right)^2.
\end{aligned}$$

In spectral language the last estimate reads as follows

$$\begin{aligned}
\left(\tilde{a}_l^{L_j}\right)^2 &= \left(w_l^{L_j}\right)^2 \sum_{n=0}^{N_j} \left(U_n^*(y_l^{L_j})\right)^2 \left(\tilde{F}^{\wedge}(n)\right)^2 \\
&\geq \left(w_l^{L_j}\right)^2 \sum_{n=0}^{N_j} \left(U_n^*(y_l^{L_j})\right)^2 K^{\wedge}(n) \\
&= \left(k_l^{L_j}\right)^2.
\end{aligned}$$

For the given threshold values $k_l^{L_j}$ a multiscale estimator ('$\hat{}$' for estimated) can be written in the form:

$$\begin{aligned}
\hat{F}_J &= \sum_{i=1}^{L_0} I_{\{(\tilde{a}_i^{L_0})^2 \geq (k_i^0)^2\}} \left(\Phi_0 *_{\mathcal{H}} \Phi_0\right)(y_i^{L_0}) \tilde{a}_i^{L_0} \\
&+ \sum_{j=0}^{J-1} \sum_{i=1}^{L_j} I_{\{(\tilde{a}_i^{L_j})^2 \geq (k_i^j)^2\}} \left(\Psi_j *_{\mathcal{H}} \Psi_j\right)(y_i^{L_i}) \tilde{a}_i^{L_i}.
\end{aligned}$$

In other words, the large coefficients (relative to the threshold $k_i^{L_j}$, $i = 1, \ldots, L_j$, $j = 0, \ldots, J-1$) are kept intact and the small coefficients are set to zero. The estimator $\hat{F}_J$ can be reformulated in the following way

$$\begin{aligned} \hat{F}_J &= \sum_{i=1}^{L_0} \delta^{hard}_{(k_i^0)} \left((\tilde{a}_i^{L_0})^2 \right) (\Phi_0 *_{\mathcal{H}} \Phi_0)\,(y_i^{L_0}) \tilde{a}_i^{L_0} \\ &+ \sum_{j=0}^{J-1} \sum_{i=1}^{L_j} \delta^{hard}_{(k_i^j)} \left((\tilde{a}_i^{L_j})^2 \right) (\Psi_j *_{\mathcal{H}} \Psi_j)\,(y_i^{L_i}) \tilde{a}_i^{L_i}, \end{aligned}$$

where the function δ_λ^{hard} is the *hard thresholding function*

$$\delta_\lambda^{hard}(\alpha) = \begin{cases} 1 & \text{if } |\alpha| \geq \lambda \\ 0 & \text{otherwise} \end{cases} .$$

The "keep or kill" hard thresholding operation is not the only reasonable way of estimating the coefficients. Recognizing that each wavelet coefficient consists of both a signal portion and a noise portion, it might be desirable to attempt to isolate the signal contribution by removing the noisy part. This idea leads to the *soft thresholding function* (see the considerations by [7, 8])

$$\delta_\lambda^{hard}(\alpha) = \begin{cases} \max\{0, 1 - \frac{\lambda}{|\alpha|}\} & \text{if } \alpha \neq 0 \\ 0 & \text{if } \alpha = 0 \end{cases} ,$$

which can also be used in the estimators stated above. When soft thresholding is applied to a set of empirical coefficients, only coefficients greater than the threshold (in absolute value) are included, but their values are 'shrunk' toward zero by an amount equal to the threshold λ.

Summarizing all our results we finally obtain the following *thresholding multiscale estimator* $\hat{F}_J$ for a function $F \in \mathcal{H}$ known from error-affected $\tilde{F}$:

$$\begin{aligned} \hat{F}_J &= \sum_{i=1}^{L_0} \delta^{hard}_{(k_i^0)} \left((\tilde{a}_i^{L_0})^2 \right) \Phi_0^{(2)}(\cdot, y_i^{L_o}) \tilde{a}_i^{L_0} \\ &+ \sum_{j=0}^{J-1} \sum_{i=1}^{L_j} \delta^{hard}_{(k_i^j)} \left((\tilde{a}_i^{L_j})^2 \right) \Psi_j^{(2)}(\cdot, y_i^{L_j}) \tilde{a}_i^{L_j}, \end{aligned}$$

where the coefficients $\tilde{a}_i^{L_j}$ are given recursively (see (53),(61)) by the formulae

$$\tilde{a}_i^{L_j} = w_i^{L_j} \sum_{l=1}^{L_{j+1}} \tilde{a}_i^{L_{j+1}} (SH)_{N_j}(y_i^{L_j}, y_i^{L_{j+1}}),\ i = 1, \ldots, L_j,\ j = 0, \ldots, J-1$$

and

$$\tilde{a}_i^{L_J} = w_i^{L_J} \tilde{F}(y_l^{L_J}),\ i = 1, \ldots, L_J.$$

In conclusion, $\hat{F}_J$ is first approximated by a thresholded $\hat{F}_0$. Then the coefficients of higher resolutions are thresholded.

11. Legendre wavelets

As a first example we consider the space $\mathrm{L}^2[-1,+1]$ of square–integrable functions $F : [-1,+1] \to \mathbb{R}$, i.e. $\Sigma = [-1,+1]$ and $\mathcal{H} = \mathrm{L}^2[-1,+1]$. The kernels resulting from this choice, i.e. Legendre scaling functions and wavelets, can be used for one–dimensional time-series analysis or, in combination with scalar or vectorial spherical wavelets, for the analysis and approximation of time dependent scalar or vector fields on the sphere. Since this subject is beyond the scope of this survey, we do not present an example and therefore keep the treatise brief.

On the space $\mathrm{L}^2[-1,+1]$ we are able to introduce, as usual, the inner product

$$(F,G)_{\mathrm{L}^2[-1,+1]} = \int_{-1}^{+1} F(t)G(t)\ dt, \quad F,G \in \mathrm{L}^2[-1,+1]. \tag{66}$$

The $\mathrm{L}^2[-1,+1]$–orthonormal Legendre polynomials P_n^*: $[-1,+1] \to \mathbb{R}$ given by

$$P_n^* = \sqrt{\frac{2n+1}{2}} P_n, \quad n = 0,1,\ldots \tag{67}$$

with

$$P_n(t) = \sum_{s=0}^{[n/2]} (-1)^s \frac{(2n-2s)!}{2^n (n-2s)!(n-s)!s!} t^{n-2s}, \quad t \in [-1,+1] \tag{68}$$

form a Hilbert basis in $\mathrm{L}^2[-1,+1]$. In other words, every $F \in \mathrm{L}^2[-1,+1]$ admits a Fourier expansion $F = \sum_{n=0}^{\infty} F^\wedge(n) P_n^*$, where the Fourier coefficients read as follows:

$$F^\wedge(n) = (F, P_n^*)_{\mathrm{L}^2[-1,+1]} = \int_{-1}^{+1} F(t) P_n^*(t)\ dt, \quad n = 0,1,\ldots. \tag{69}$$

The $\mathrm{L}^2[-1,+1]$–admissible product kernels (cf. [3]) are given by

$$\Gamma(x,t) = \sum_{n=0}^{\infty} \Gamma^\wedge(n) P_n^*(x) P_n^*(t), \quad x,t \in [-1,+1] \tag{70}$$

with $\Gamma^\wedge(n) \in \mathbb{R}$, $n \in \mathbb{N}_0$, where the symbol of the $\mathrm{L}^2[-1,1]$–kernel has to satisfy the estimates

$$(i) \quad \sum_{n=0}^{\infty} (\Gamma^\wedge(n))^2 < \infty, \qquad (ii) \quad \sum_{n=0}^{\infty} (\Gamma^\wedge(n) P_n^*(t))^2 < \infty \tag{71}$$

for all $t \in [-1,+1]$. A sufficient condition for the validity of the conditions (i) and (ii) in (71) is given by

$$\sum_{n=0}^{\infty} (\Gamma^{\wedge}(n))^2 \frac{2n+1}{4\pi} < \infty \tag{72}$$

(note that $|P_n(t)| \leq 1$ for all $t \in [-1,+1]$).

Let $\{(\Phi_j)^{\wedge}(n)\}_{n=0,1,\ldots}$, $j \in \mathbb{Z}$, be the generating symbol of a scaling function $\{\Phi_j\}$. Then $\lim_{J\to\infty} \|F_J - F\|_{\mathbb{L}^2[-1,+1]} = 0$ holds for all $F \in \mathbb{L}^2[-1,+1]$, where the J–level approximation F_J is given by

$$F_J = \int_{-1}^{+1} \Phi_J(\cdot,x) \int_{-1}^{+1} \Phi_J(x,t)F(t)\ dt\ dx = \int_{-1}^{+1} \Phi_J^{(2)}(\cdot,t)F(t)\ dt. \tag{73}$$

The scale spaces $\mathcal{V}_j$ are given by

$$\mathcal{V}_j = \left\{ \int_{-1}^{+1} \Phi_j^{(2)}(\cdot,t)F(t)\ dt \middle| F \in \mathbb{L}^2[-1,+1] \right\}, \tag{74}$$

while the detail spaces are of the form

$$\mathcal{W}_j = \left\{ \int_{-1}^{+1} \Psi_j^{(2)}(\cdot,t)F(t)\ dt \middle| F \in \mathbb{L}^2[-1,+1] \right\}. \tag{75}$$

The wavelet transform WT at scale j and position $x \in [-1,+1]$ reads as follows:

$$(WT)(F)(j;x) = \int_{-1}^{+1} \Psi_j(x,t)F(t)\ dt, \quad F \in \mathbb{L}^2[-1,+1]. \tag{76}$$

Finally, the reconstruction formula of $F \in \mathbb{L}^2[-1,+1]$ allows the (bilinear) representation

$$\begin{aligned} F &= \int_{-1}^{+1} \Phi_0(\cdot,x) \int_{-1}^{+1} \Phi_0(x,t)F(t)\ dt\ dx \\ &\quad + \sum_{j=0}^{\infty} \int_{-1}^{+1} \Psi_j(\cdot,x)(WT)(F)(j;x)\ dx\,. \end{aligned}$$

12. Spherical wavelets

As reference space we now use the space $\mathcal{L}^2(\Omega)$ of square–integrable functions $F : \Omega \to \mathbb{R}$ on the unit sphere Ω in three–dimensional Euclidean space $\mathbb{R}^3$ (i.e.: $\Sigma = \Omega \subset \mathbb{R}^3$ and $\mathcal{H} = \mathcal{L}^2$). We consider $\mathcal{L}^2$ to be equipped with the inner product $(F,G)_{\mathcal{L}^2} = \int_\Omega F(\xi)G(\xi)d\omega(\xi)$, $F,G \in \mathcal{L}^2$ ($d\omega$ is the surface element). As $\mathcal{L}^2$–orthonormal system

we choose the system $\{Y_{n,k}\}_{\substack{n=0,1,\dots,\\ k=1,\dots,2n+1}}$ of spherical harmonics $Y_{n,k}$ of degree n and order k (see e.g. [10, 11] for more details). From the addition theorem we know that

$$\sum_{k=1}^{2n+1} Y_{n,k}(\xi)Y_{n,k}(\eta) = \frac{2n+1}{4\pi}P_n(\xi\cdot\eta), \quad \xi,\eta\in\Omega, \tag{77}$$

where P_n is the Legendre polynomial (67) of degree n.

Clearly, every function $F\in\mathcal{L}^2$ can be represented in the form $F=\sum_{n=0}^{\infty}\sum_{k=1}^{2n+1}F^\wedge(n,k)Y_{n,k}$, where the Fourier coefficients are given by $F^\wedge(n,k)=(F,Y_{n,k})_{\mathcal{L}^2}=\int_\Omega F(\eta)Y_{n,k}(\eta)d\omega(\eta)$. The $\mathcal{L}^2$–product kernels (cf. [10, 11])are of the form

$$\Gamma(\xi,\eta)=\sum_{n=0}^{\infty}\sum_{k=1}^{2n+1}\Gamma^\wedge(n,k)Y_{n,k}(\xi)Y_{n,k}(\eta) \tag{78}$$

with $\Gamma^\wedge(n,k)\in\mathbb{R}$ for $n=0,1,\dots;k=1,\dots,2n+1$, where

$$\sum_{n=0}^{\infty}\sum_{k=1}^{2n+1}(\Gamma^\wedge(n,k))^2\frac{2n+1}{4\pi}<\infty \tag{79}$$

is a sufficient condition for the admissibility (i) and (ii) (note that $|Y_{n,k}(\xi)|\le\sqrt{(2n+1)/4\pi}$ for all $\xi\in\Omega$). In case of rotational invariance, i.e. $\Gamma^\wedge(n,k)=\Gamma^\wedge(n)$ for $n=0,1,\dots;\ k=1,\dots,2n+1$, the conditions (i) and (ii) reduce to

$$\sum_{n=0}^{\infty}(\Gamma^\wedge(n))^2\frac{2n+1}{4\pi}<\infty\ . \tag{80}$$

The convolution of Γ against F is canonically understood by

$$\begin{aligned}(\Gamma *_{\mathcal{L}^2} F)(\xi) &= (\Gamma(\xi,\cdot),F)_{\mathcal{L}^2} \\ &= \int_\Omega \Gamma(\xi,\eta)F(\eta)d\omega(\eta) \\ &= \sum_{n=0}^{\infty}\sum_{k=1}^{2n+1}\Gamma^\wedge(n,k)F^\wedge(n,k)Y_{n,k}(\xi),\quad \xi\in\Omega\ .\end{aligned} \tag{81}$$

Let $\{(\Phi_J)^\wedge(n,k)\}_{\substack{n=0,1,\dots\\ k=1,\dots,2n+1}}$, $J\in\mathbb{Z}$, be the generating symbol of a scaling function $\{\Phi_J\}$. Then we have $\lim_{J\to\infty}\|F_J-F\|_{\mathcal{L}^2}=0$ for all $F\in\mathcal{L}^2$, where F_J is given by $F_J=\int_\Omega\Phi_J^{(2)}(\cdot,\eta)F(\eta)\ d\omega(\eta)$. The scale and detail spaces and the wavelet transform WT are given in canonical way.

The reconstruction formula recovering a function $F\in\mathcal{L}^2$ now reads

$$F=\int_\Omega\Phi_0^{(2)}(\cdot,\eta)F(\eta)\ d\omega(\eta)+\sum_{j=0}^{\infty}\int_\Omega\Psi_j^{(2)}(\cdot,\eta)F(\eta)d\omega(\eta)\,. \tag{82}$$

Again, the Shannon kernel $(SH)_{2^j-1}$ admits an explicit representation. The space $\mathcal{V}_j$ is equivalent to the space $\mathcal{H}_{0,\ldots,2^j-1} = Pol_{2^j-1}(\Omega)$ of restrictions to Ω of (homogeneous harmonic) polynomials in $\mathbb{R}^3$ of degree $\leq 2^j-1$. The dimension of $Pol_{2^j-1}(\Omega)$ is equal to $\sum_{n=0}^{2^j-1}(2n+1) = (2^j)^2 = 2^{2j}$.

For $j = 0,\ldots,J$, the generating coefficients $w_l^{L_j} \in \mathbb{R}$ and nodal points $\eta_l^{L_j} \in \Omega$, $l = 1,\ldots,L_j$, of polynomial exact integration formulae of degree $L_j \geq 2(2^j-1)$ are calculable from the linear systems

$$\int_\Omega (SH)_{L_j}(\xi,\eta_i^{L_j})d\omega(\xi) = \sum_{l=1}^{L_j} w_l^{Lj}(SH)_{L_j}(\eta_i^{L_j},\eta_l^{L_j}) \tag{83}$$

$i = 1,\ldots,L_j$ (note that the matrix $((SH)_{2^j-1}(\eta_i^{L_j}.\eta_l^{L_j}))_{i,l=1,\ldots,}$ is assumed to be of maximal rank). Again we are able to make profit of the fact that $\Phi_j^{(2)}(\cdot,\xi) \in Pol_{2^j-1}(\Omega)$ and $\int_\Omega (SH)_{2^j-1}(\cdot,\eta)F(\eta)d\omega(\eta) \in Pol_{2^j-1}(\Omega)$, hence, (as a function of ξ) $\Phi_j^{(2)}(\cdot,\xi)\int_\Omega (SH)_{2^j-1}(\xi\cdot\eta)F(\eta)\,d\omega(\eta) \in Pol_{2^{j+1}-2}(\Omega)$ (for more details on polynomial exact integration the reader is e.g. referred to [10, 11, 16]). In conclusion, we get

$$\begin{aligned}&\int_\Omega (\Phi_j^{(2)})(\cdot,\xi)\int_\Omega (SH)_{2^j-1}(\xi,\eta)F(\eta)d\omega(\eta) \\ &= \sum_{l=1}^{L_j} w_l^{L_j}\Phi_j^{(2)}(\cdot,\eta_l^{L_j})\int_\Omega (SH)_{2^j}(\eta_l^{L_j},\eta)F(\eta)d\omega(\eta)\ .\end{aligned} \tag{84}$$

$j = 0,\ldots,J$. The J–level approximation F_J can be obtained in recursive way via the tree algorithm (pyramid scheme) as indicated in this paper.

For illustrational purposes we present some results obtained by using spherical wavelets for noise cancellation. Using the well known NASA, GSFC and NIMA EGM96 model (see http://cddisa.gsfc.nasa.gov/926/egm96/egm96.html) for the gravitational potential we calculated a potential function including contributions of spherical harmonic degrees 3 up to 127. This function was evaluated on the 66564 nodal points of a point system suitable for numerical integration (see [9] for details on the point system and the integration technique used). We then 'contaminated' this data set with bandlimited white noise of variance $\sigma^2 \simeq 14.4$ and bandwidth $n_K \simeq 257$. This resulted in noise of the order of magnitude 10^2 [Gal m] in a field of the order of magnitude 10^4 [Gal m]. Note that bandlimited white noise is characterized by the following symbol of the covariance kernel function:

$$K^\wedge(n) = \begin{cases} \frac{\sigma^2}{(n_K+1)^2} & , \quad n \leq n_K, \\ 0 & , \quad n > n_K, \end{cases}\ .$$

It should be remarked that, when looking at the pictures, the noise is not constant at the poles as one should expect it to be. This is due to our routine of adding the noise

to the synthetic data. However, our results are not influenced by this, since during the process of decomposition and reconstruction each data point of the rectangular domain is weighted by corresponding integration weights which are constructed such that the poles do not contribute to the whole integration. The denoising process has been carried out using Shannon wavelets from scales j=0 to 6 and the hard thresholding criterion. Figure 1 shows the gravitational potential after the denoising process, Figures 2 and 3 show the noise in the data before and after the noise cancellation, respectively. The rms error of the noisy data-set w.r.t. the clean data has been improved by 51 per cent. Because of the space localizing properties of the wavelets, local calculations become possible. Figure 4 shows the result of a locally denoised data set, i.e. from the global data distribution we have extracted a local data set over South America and applied our algorithms to this spatially restricted area. This resulted in an improvement of the rms error of 31 per cent.

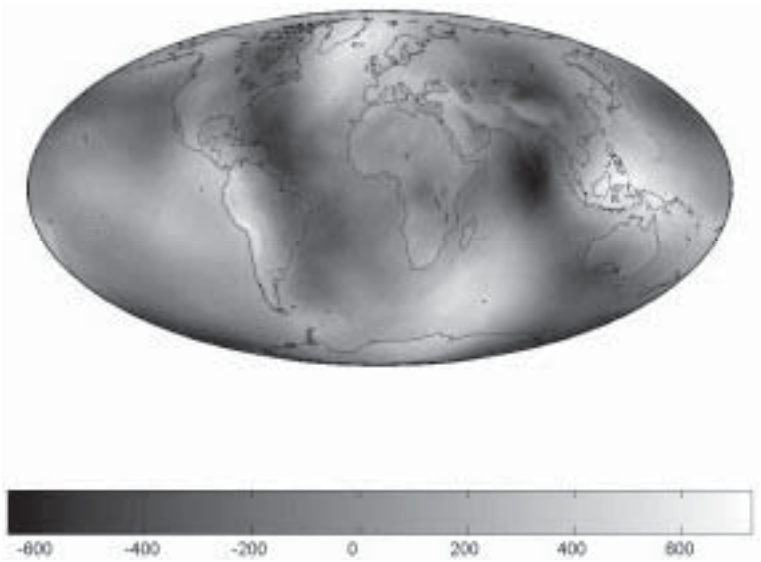

Figure 1: Denoised graviational potential [100 Gal m]

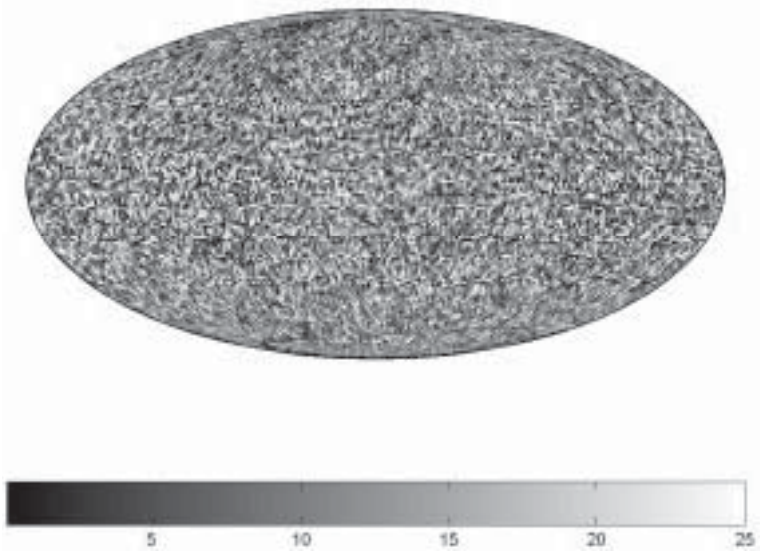

Figure 2: Noise before the denoising process [100 Gal m]

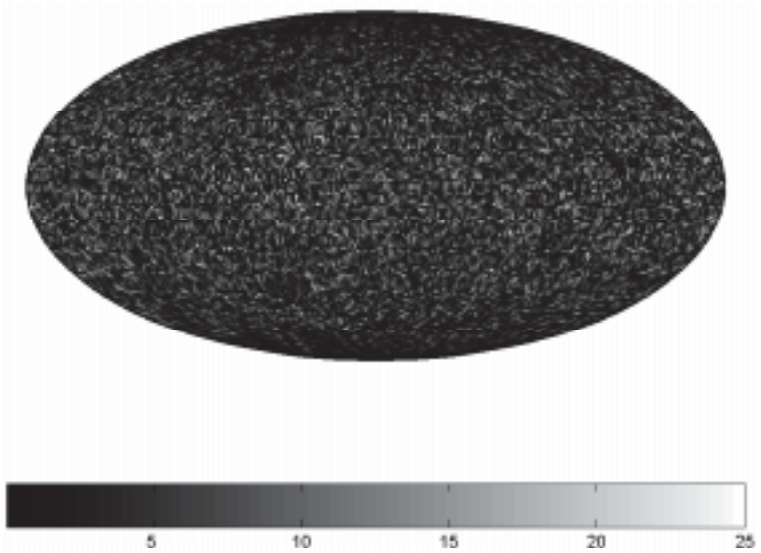

Figure 3: Noise after the denoising process [100 Gal m]

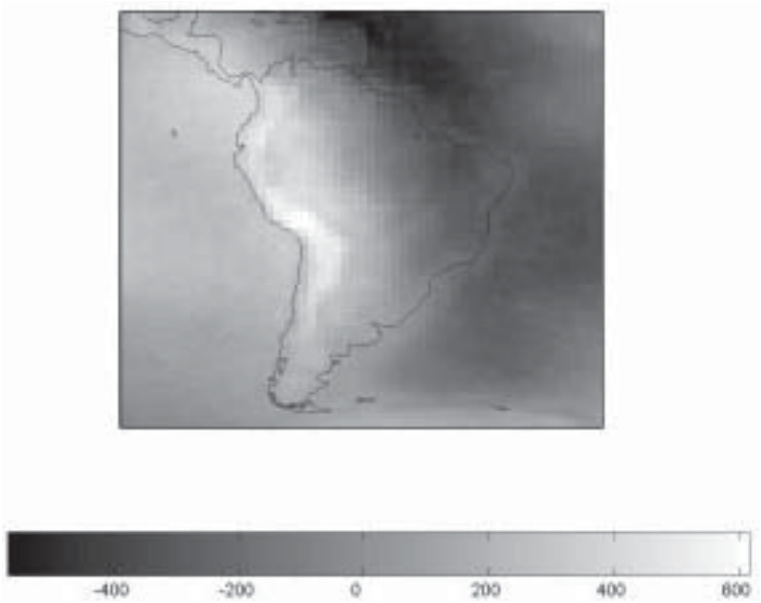

Figure 4: Denoised graviational potential over South America [100 Gal m]

Last but not least we present a computational example illustrating the concept of multiresolution analysis. The multiresolution analysis 'looks at' the given data (in this case the EGM96 model potential up to degree and order 360) through a magnifying-glass, the resolution of which gets finer and finer. Thus it associates to the potential a sequence of smoothed versions, labelled by the scale parameter j. These aspects are illustrated in the Figures 6 to 11. The computations have been accomplished using CP scaling functions and wavelets. The nodal points and the corresponding weights needed for the numerical integration are chosen as described in [16].

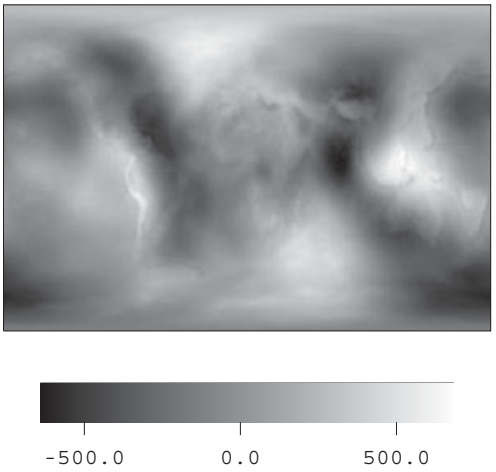

Figure 5: raw data set [100 Gal]

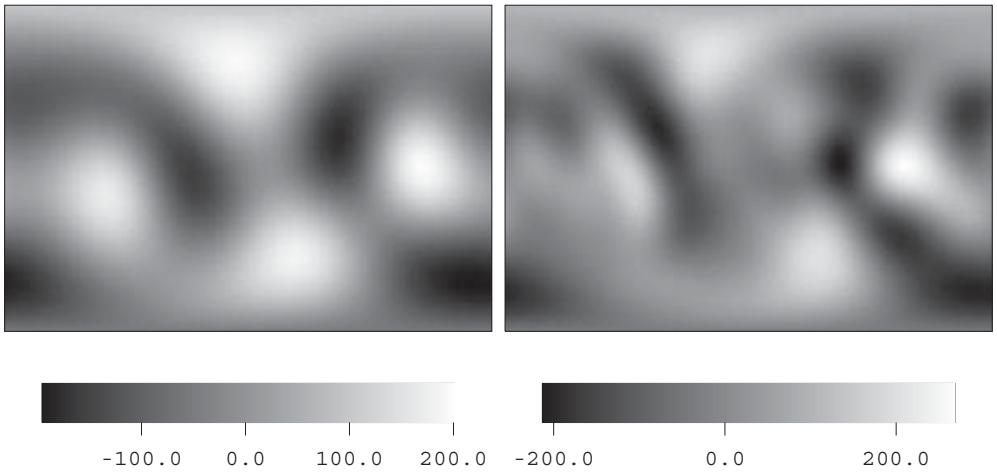

Figure 6: $T_3(F)$ (left) and $R_3(F)$ (right) in [100 Gal]

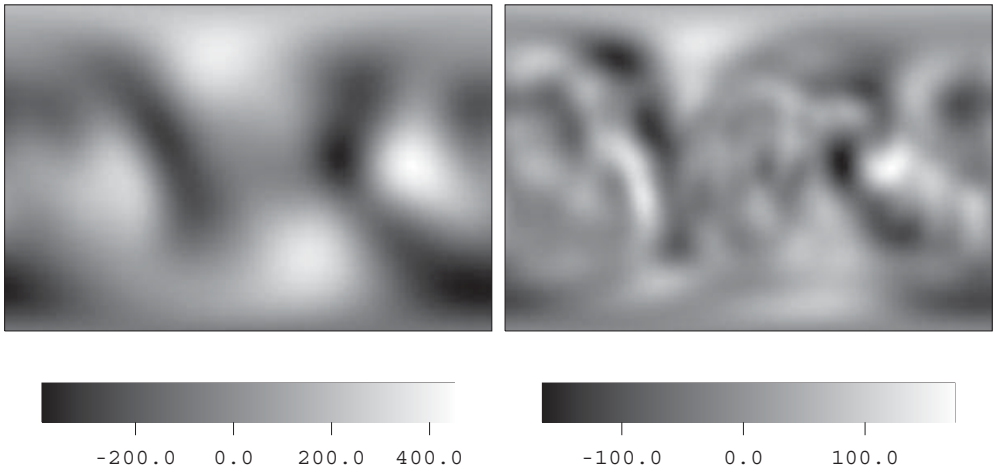

Figure 7: $T_4(F)$ (left) and $R_4(F)$ (right) in [100 Gal]

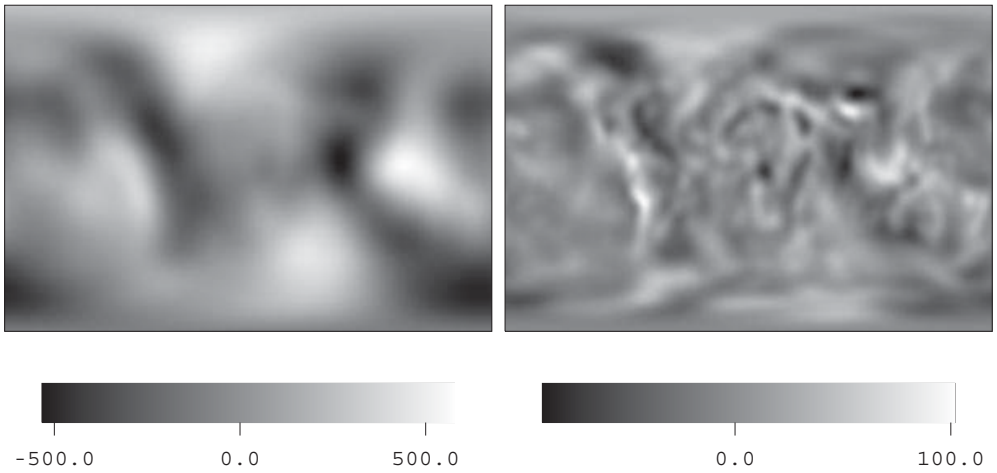

Figure 8: $T_5(F)$ (left) and $R_5(F)$ (right) in [100 Gal]

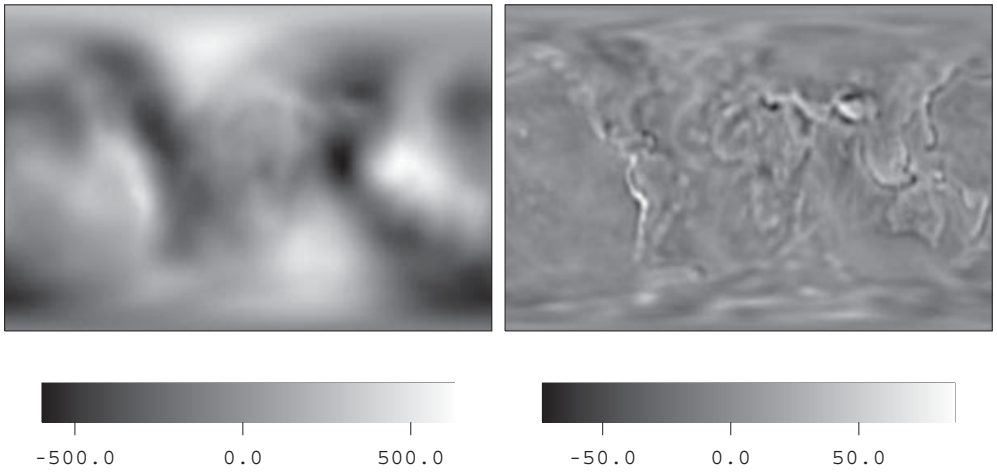

Figure 9: $T_6(F)$ (left) and $R_6(F)$ (right) in [100 Gal]

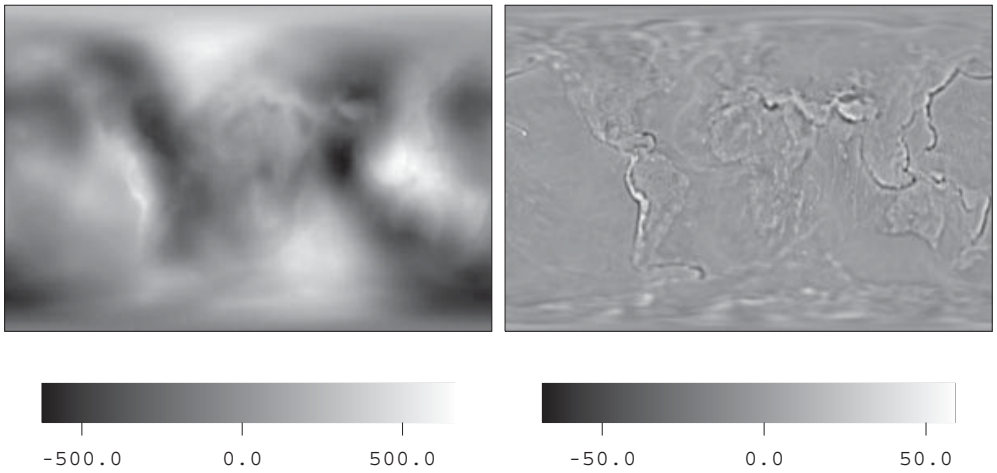

Figure 10: $T_7(F)$ (left) and $R_7(F)$ (right) in [100 Gal]

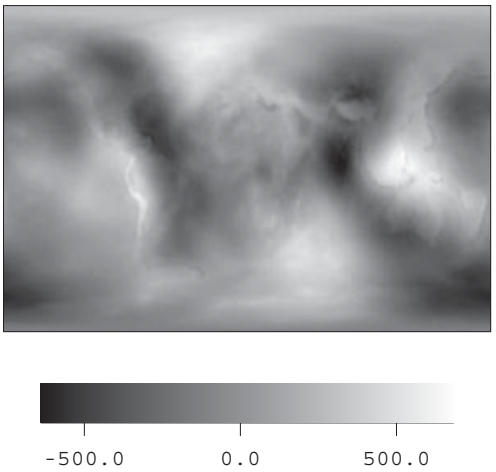

Figure 11: $T_8(F)$ [100 Gal]

13. Spherical vectorial wavelets

Now we consider the space $l^2(\Omega)$ of square-integrable vectorial functions $f : \Omega \to \mathbb{R}^3$ on the unit sphere (i.e. $\Sigma = \Omega \subset \mathbb{R}^3$, $\mathcal{H} = l^2(\Omega)$). Equipped with the inner product $(f,g)_{l^2(\Omega)} = \int_\Omega f(\eta) \cdot g(\eta)\, d\omega(\eta)$, $f, g \in l^2(\Omega)$, $l^2(\Omega)$ is a Hilbert space. Using the $\mathcal{L}^2$-orthonormal system $\{Y_{n,k}\}_{\substack{n=0,1,\dots \\ k=1,\dots,2n+1}}$ of spherical harmonics (see Section 12) we are able to introduce an $l^2(\Omega)$-orthonormal system $\{y_{n,k}^{(i)}\}_{\substack{n=0_i,1,\dots \\ k=1,\dots,2n+1}}^{i=1,2,3}$ via

$$y_{n,k}^{(1)}(\xi) = \xi Y_{n,k}(\xi), \tag{85}$$

$$y_{n,k}^{(2)}(\xi) = \frac{1}{\sqrt{(n(n+1))}} \nabla_\xi^* Y_{n,k}(\xi), \tag{86}$$

$$y_{n,k}^{(3)}(\xi) = \frac{1}{\sqrt{(n(n+1))}} L_\xi^* Y_{n,k}(\xi), \tag{87}$$

where $\xi \in \Omega$, ∇_ξ^* is the surface gradient and $L_\xi^* = \xi \wedge \nabla_\xi^*$ is the surface curl gradient (see [11] for more details), $0_i = 0$ for $i = 1$ and $0_i = 1$ for $i = 2, 3$. Using $\{y_{n,k}^{(i)}\}_{\substack{n=0_i,1,\dots \\ k=1,\dots,2n+1}}^{i=1,2,3}$ every function $f \in l^2(\Omega)$ can be represented by its orthogonal expansion, i.e.

$$f = \sum_{i=1}^{3} \sum_{n=0_i}^{\infty} \sum_{k=1}^{2n-1} (f^{(i)})^\wedge(n,k) y_{n,k}^{(i)} \tag{88}$$

with coefficients $(f^{(i)})^\wedge(n,k) = \int_\Omega f(\eta)\cdot y_{n,k}^{(i)}(\eta)\,d\omega(\eta)$. The vectorial $l^2(\Omega)$ kernel functions of type i are of the form

$$\Gamma^{(i)}(\xi,\eta) = \sum_{n=0_i}^{\infty}\sum_{k=1}^{2n+1}(\Gamma^{(i)})^\wedge(n)y_{n,k}^{(i)}(\xi)Y_{n,k}(\eta), \tag{89}$$

and the vectorial $l^2(\Omega)$ kernel functions are then derived by

$$\Gamma(\xi,\eta) = \sum_{i=1}^{3}\Gamma^{(i)}(\xi,\eta), \tag{90}$$

with $(\Gamma^{(i)})^\wedge(n)\in\mathbb{R}$ for $i=1,2,3$, $n=0,1,\ldots$ (see [1]). Admissibility is guaranteed provided that

$$\sum_{n=0_i}^{\infty}\left((\Gamma^{(i)})^\wedge(n)\right)^2\frac{2n+1}{4\pi}<\infty \tag{91}$$

is assumed. It should be observed that, if P_n denotes the Legendre polynomial of degree n, $\nabla_\xi^* P_n(\xi\cdot\eta) = (\eta-(\xi\cdot\eta)\xi)P_n'(\xi\cdot\eta)$ and $L_\xi^* P_n(\xi\cdot\eta) = \xi\wedge\eta P_n'(\xi\cdot\eta)$, such that singularities at the poles are completely avoided by use of the kernel representations (89). In connection with the addition theorem (77) of scalar spherical harmonics this leads to the following, numerically very useful, representations of the vectorial kernel functions of type i:

$$\Gamma^{(1)}(\xi,\eta) = \xi\sum_{n=0_i}^{\infty}\sum_{k=1}^{2n+1}\frac{2n+1}{4\pi}(\Gamma^{(1)})^\wedge(n)P_n(\xi\cdot\eta) \tag{92}$$

$$\Gamma^{(2)}(\xi,\eta) = (\eta-(\xi\cdot\eta)\xi)\sum_{n=0_i}^{\infty}\sum_{k=1}^{2n+1}\frac{2n+1}{4\pi\sqrt{n(n+1)}}(\Gamma^{(2)})^\wedge(n)P_n'(\xi\cdot\eta) \tag{93}$$

$$\Gamma^{(3)}(\xi,\eta) = (\xi\wedge\eta)\sum_{n=0_i}^{\infty}\sum_{k=1}^{2n+1}\frac{2n+1}{4\pi\sqrt{n(n+1)}}(\Gamma^{(3)})^\wedge(n)P_n'(\xi\cdot\eta) \tag{94}$$

The following concept of convolutions is not totally reflected by the general Hilbert space approach discussed in the previous chapters, but it is still in quite analogy to the presented wavelet idea:
Using the kernels (92),(93) and (94), two kinds of convolutions will be introduced (cf. [1]), i.e. a convolution of vectorial kernels against vectorial functions - resulting in scalar coefficients - and a convolution of vectorial kernels against scalar valued functions - enabling us to reconstruct a vectorial function from scalar coefficients. The corresponding convolutions are given by

$$(\Gamma * f)(\xi) = \int_\Omega \Gamma(\eta,\xi)\cdot f(\eta)\,d\omega(\eta)$$

$$= \sum_{i=1}^{3} \sum_{n=0_i}^{\infty} \sum_{k=1}^{2n+1} (f^{(i)})^{\wedge}(n,k) Y_{n,k}(\xi), \quad \xi \in \Omega,$$

mapping vector fields onto scalar fields and

$$\begin{aligned} (\Gamma \star F)(\xi) &= \int_{\Omega} \Gamma(\xi,\eta) F(\eta)\, d\omega(\eta) \\ &= \sum_{i=1}^{3} \sum_{n=0_i}^{\infty} \sum_{k=1}^{2n+1} F^{\wedge}(n,k) y_{n,k}^{(i)}(\xi), \quad \xi \in \Omega, \end{aligned}$$

mapping scalar functions onto vectorial functions. Applying both convolutions consecutively to a function $f \in l^2$ results in

$$(\Gamma \star \Gamma * f)(\xi) = \sum_{i=1}^{3} \sum_{n=0_i}^{\infty} \sum_{k=1}^{2n+1} ((\Gamma^{(i)})^{\wedge}(n))^2 (f^{(i)})^{\wedge}(n,k) y_{n,k}^{(i)}(\xi) \quad \xi \in \Omega. \tag{95}$$

Hence, the reconstruction formula recovering a function $f \in l^2$ now reads

$$f = \Phi_0 \star \Phi_0 * f + \sum_{j=0}^{\infty} \Psi_j \star \Psi_j * f \tag{96}$$

with $\Phi_0 = \sum_{i=1}^{3} \Phi_0^{(i)}$ and $\Psi_j = \sum_{i=1}^{3} \Psi_j^{(i)}$. Again, as in the scalar case one can make use of discretizations of integrals and use efficient pyramid schemes.

Once again, strictly spoken, this approach is a slight extension to the general concept since here two different types of convolutions are defined. This, however, is based on the fact that the direct application of the general approach to vector fields would involve tensorial kernel functions. Though being the canonical approach in the sense of this review, the tensorial kernel functions hold some disadvantages for numerical applications and will be omitted here (for more details see [1] and [11]).

Similar to the scalar case, we present here an illustrative application of vectorial spherical wavelets for the denoising of spherical vector fields. From a bandlimited geomagnetic potential up to degree 13 (see [4]) we calculated the corresponding gradient field w.r.t. a local moving triad of unit vectors $\{\varepsilon^t, \varepsilon^\varphi, \varepsilon^r\}$, where $t \in [-1,1]$ is the polar distance, $\varphi \in [-\pi, \pi)$ is the spherical longitude and r is the radius of the sphere of interest (e.g. a satellite orbit in spherical approximation). For details on notation the reader is referred to [11]. In similarity to the scalar example given above, we computed the gradient field on 3600 nodal points of a suitable integration point system (cf. [9]) (note that, due to the lower degree of the geomagnetic potential we need less integration points). In a second step each vectorial component was "contaminated" with bandlimited white noise of bandlimit n_K and variance σ^2 of approximately 60

and 0.9, respectively (see the remarks in Section 12). This resulted in noise of the order of magnitude 10^0 [nT] in field components of the order of magnitude 10^4 [nT]. The denoising process has been accomplished using vectorial Shannon wavelets of type 1 and 2 and of scales $j = 1$ to 3 and applying the hard thresholding criterion. Figure 12 show the denoised negative radial component (i.e. the $-\varepsilon^r$-component) and the denoised tangential ε^φ-component of the gradient field (the results for the ε^t are similar and are therefore omitted). Figure 13 shows the noise that has been added to the field components (see the remarks in Section 12) while Figure 14 shows the remaining noise after the noise cancellation. The rms error w.r.t. the unnoised data has been improved by 87 per cent for the $-\varepsilon^r$-component and by 89 per cent for the ε^φ-component.

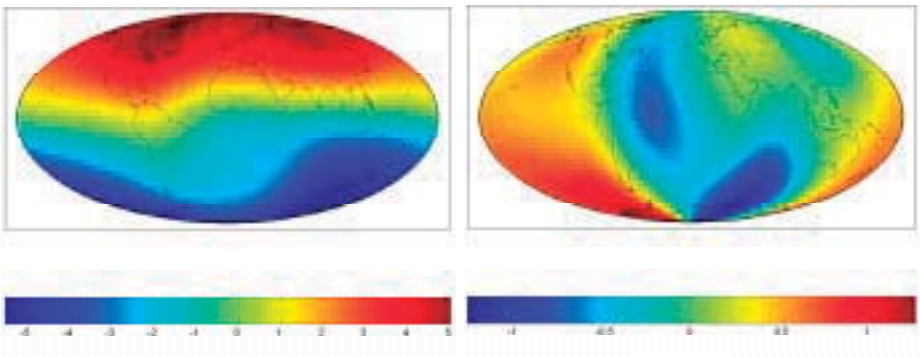

Figure 12: Denoised $-\varepsilon^r$-component (left) and ε^φ-component in 10000 [nT]

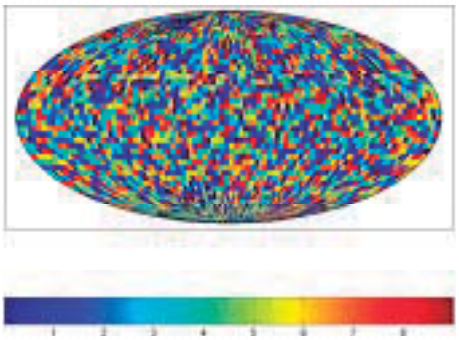

Figure 13: Absolute value of noise [nT]

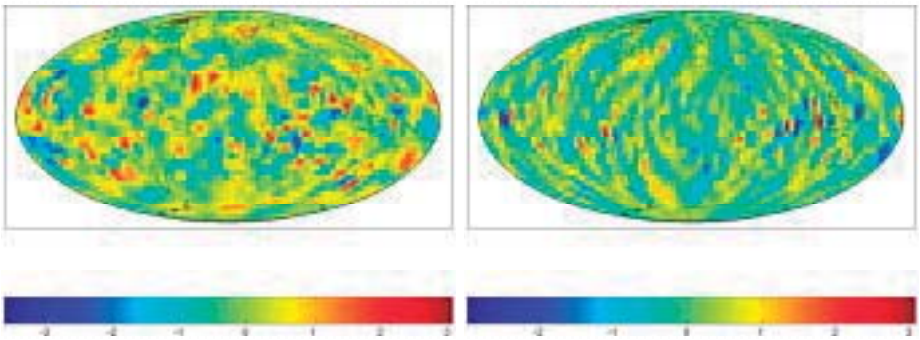

Figure 14: Error of denoised $-\varepsilon^r$ (left) and ε^φ (right) component w.r.t. clear data [nT]

Finally we close with an example of spherical vectorial wavelets applied to CHAMP Fluxgate-magnetometer data. CHAMP is a geoscientific satellite run by the GeoForschungsZentrum (GFZ) in Potsdam, Germany (see http://www.gfz-potsdam.de and www.gfz-potsdam.de/champ/ for more information on the GFZ or the CHAMP satellite mission). In addition to gravitational field and ionospheric measurements, CHAMP is designed to map the geomagnetic field with high accuracy using a scalar Overhauser-magnetometer and two vector Fluxgate-magnetometers. In the following example we have applied spherical vectorial wavelets to vector data from August 2001 to November 2001 (10:00 - 16:00 local time). In a first step the data have been corrected for so-called main field distributions by using the spherical harmonic model Oersted-10b-01 (cf. [15]) and have then been gridded to a regular grid using an inverse-distance method. We then have performed a vectorial multiresolution analysis using type $i = 3$ Shannon wavelets. This procedure leads to a multiresolution analysis of the so-called toroidal magnetic field at satellite height. The toroidal field is purely tangential and can be shown to be due to radial electric current distributions crossing the satellite's track (see e.g. [2]). Figures 15 up to 17 present the absolute value of the toroidal field at different scales. It can clearly be seen that in higher scales we get large contributions in the vicinity of the north- and southpole. These are due to strong current systems flowing onto and away from the Earth in the polar areas (field aligned currents).

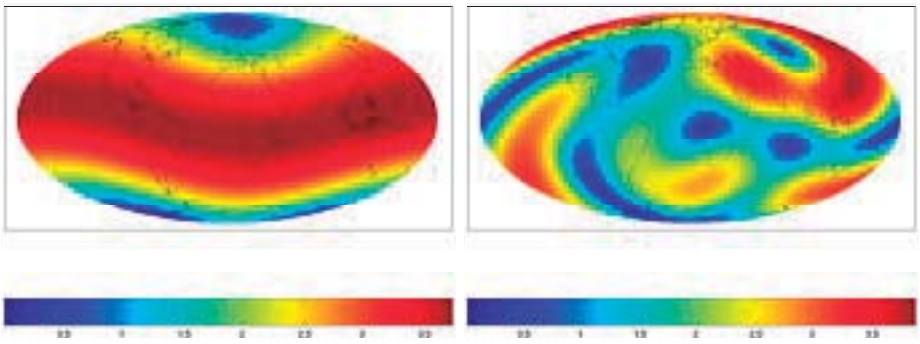

Figure 15: Toroidal Intensity at scales 0 (left) and 1 (right); [nT]

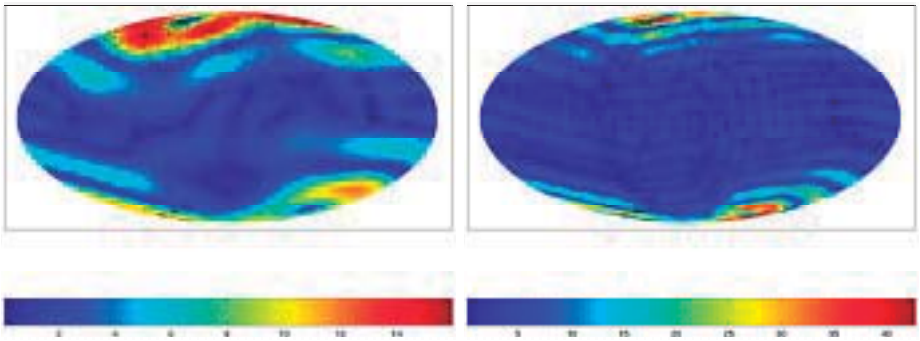

Figure 16: Toroidal Intensity at scales 2 (left) and 3 (right); [nT]

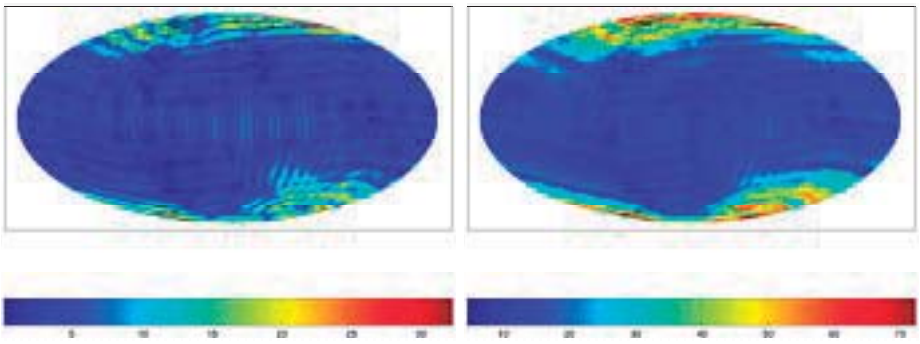

Figure 17: Toroidal Intensity at scale 4 (left) and Reconstruction (right); [nT]

Acknowledgements The support by the German Research Foundation (DFG contract No. FR 761-10-1) is gratefully acknowledged.

References

[1] M. Bayer, S. Beth, W. Freeden, (1998) Geophysical Field Modelling by Multiresolution Analysis. Acta Geod. Geoph. Hung., **33**, 289-319.

[2] M. Bayer, W. Freeden, T. Maier, (2001) A Vector Wavelet Approach to Iono- and Magnetospheric Geomagnetic Satellite Data. J. Atmos. Sol.-Terr. Phy., **63**, 581-597

[3] S. Beth, M. Viell, (1998) Uni– und multivariate Legendre Wavelets und ihre Anwendungen zur Bestimmung des Brechungsindexgradienten. In: Progress in Geodetic Science, W. Freeden (ed.), 25–33, Shaker Verlag, Aachen.

[4] C.J. Cain, D.R. Schmitz, L. Muth, (1984) Small-Scale Features in the Earth's Magnetic Field Observed by MAGSAT. Journal of Geophysical Research, Vol. 89, NO. B2, 1070-1076.

[5] C.K. Chui, (1992) An Introduction to Wavelets. Academic Press, San Diego, London.

[6] P.J. Davis, (1965) Interpolation and Approximation. Blaisdell Publishing Company, New York, Toronto, London.

[7] D.L. Donoho, I.M. Johnstone, (1994) Ideal Spatial Adaptation by Wavelet Shrinkage. Biometrika, **81**, 425–455.

[8] D.L. Donoho, I.M. Johnstone, (1995) Adapting to Unknown Smoothness Via Wavelet Shrinkage. J. Amer. Statistical Association, **90**, 1200–1224.

[9] J.R. Driscoll, D.M. Healy, (1994) Computing Fourier Transforms and Convolutions on the 2-Sphere. Adv. Appl. Math., **15**, 202-250.

[10] W. Freeden, (1999) Multiscale Modelling of Spaceborne Geodata. B.G. Teubner, Stuttgart, Leizpig.

[11] W. Freeden, T. Gervens, M. Schreiner, (1998) Constructive Approximation on the Sphere (With Applications to Geomathematics). Oxford Science Publications, Clarendon Press.

[12] W. Freeden, O. Glockner, R. Litzenberger, (1999) A General Hilbert Space Approach to Wavelets and Its Applications in Geopotential Determination. Numer. Funct. Anal. and Optimiz., **20**, 853–879.

[13] N.N. Lebedew, (1973) Spezielle Funktionen und ihre Anwendung. BI-Wissenschaftsverlag, Mannheim, Wien, Zürich.

[14] R.T. Ogden, (1997) Essential Wavelets for Statistical Applications and Data Analysis, Birkhäuser, Boston, Basel, Berlin.

[15] N. Olsen, (2002) A Model of the Geomagnetic Field and its Secular Variation for Epoch 2000 Estimated From Orsted Data. Geophys. J. Int. **149**, 453–462.

[16] I.H. Sloan, R.S. Womersley, (2000) Constructive Polynomial Approximation on the Sphere. J. Approx. Theory, **103**, 91–118.

[17] J.B. Weaver, X. Yansun, D.M. Jr., Healy, L.D. Cromwell, (1991) Filtering Noise From Images With Wavelet Transforms. Magnetic Resonance in Medicine, **24**, 288-295.